Cell Reports, Volume *38*

Supplemental information

Methylene-bridge tryptophan fatty acylation regulates PI3K-AKT signaling and glucose uptake

Song-Hua Hu, Xia-Di He, Ji Nie, Jun-Li Hou, Jiang Wu, Xiao-Yan Liu, Yun Wei, Hui-Ru Tang, Wen-Xing Sun, Shu-Xian Zhou, Yi-Yuan Yuan, Yan-Peng An, Guo-Quan Yan, Yan Lin, Peng-Cheng Lin, Jean J. Zhao, Ming-Liang Ye, Jian-Yuan Zhao, Wei Xu, and Shi-Min Zhao

Figure S1

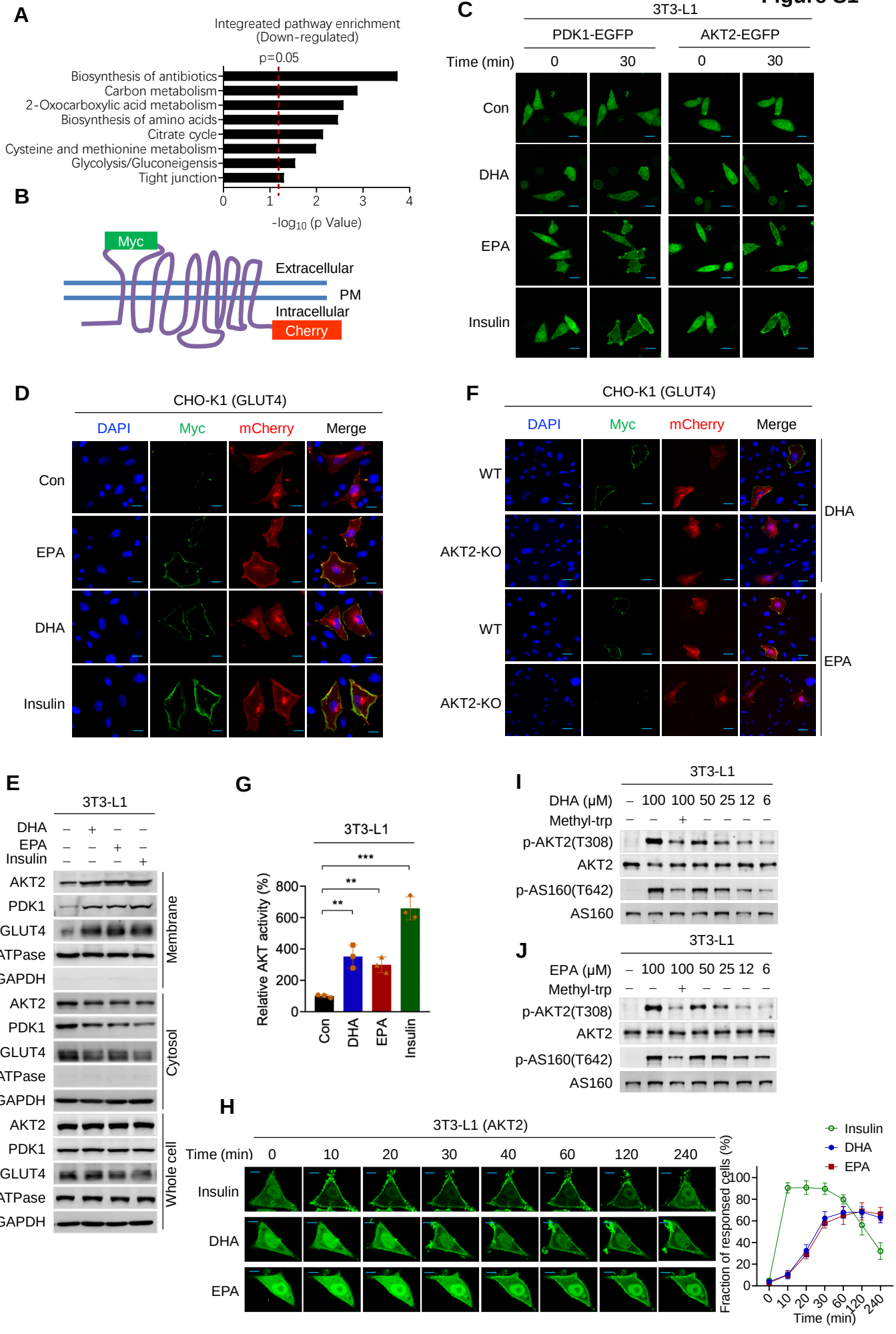
A
Integrated pathway enrichment
(Down-regulated)
p=0.05
Biosynthesis of antibiotics
Carbon metabolism
2-Oxocarboxylic acid metabolism
Biosynthesis of amino acids
Citrate cycle
Cysteine and methionine metabolism
Glycolysis/Gluconeigensis
Tight junction
0 1 2 3 4
-log10 (p Value)
B
Myc
Extracellular
PM
Intracellular
Cherry
C
3T3-L1
PDK1-EGFP
AKT2-EGFP
Time (min) 0 30 0 30
Con
DHA
EPA
Insulin
D
CHO-K1 (GLUT4)
DAPI Myc mCherry Merge
Con
EPA
DHA
Insulin
F
CHO-K1 (GLUT4)
DAPI Myc mCherry Merge
WT
AKT2-KO
WT
AKT2-KO
DHA
EPA
E
3T3-L1
DHA – + – –
EPA – – + –
Insulin – – – +
AKT2
PDK1
GLUT4
Na-K-ATPase
GAPDH
Membrane
AKT2
PDK1
GLUT4
Na-K-ATPase
GAPDH
Cytosol
AKT2
PDK1
GLUT4
Na-K-ATPase
GAPDH
Whole cell
G
3T3-L1
Relative AKT activity (%)
0 200 400 600 800
**
**
***
Con
DHA
EPA
Insulin
I
3T3-L1
DHA (μM) – 100 100 50 25 12 6
Methyl-trp – – + – – – –
p-AKT2(T308)
AKT2
p-AS160(T642)
AS160
J
3T3-L1
EPA (μM) – 100 100 50 25 12 6
Methyl-trp – – + – – – –
p-AKT2(T308)
AKT2
p-AS160(T642)
AS160
H
3T3-L1 (AKT2)
Time (min) 0 10 20 30 40 60 120 240
Insulin
DHA
EPA
Insulin
DHA
EPA
Fraction of responsed cells (%)
0 20 40 60 80 100
0 10 20 30 60 120 240
Time (min)

Figure S1 , EPA and DHA promote membrane enrichment of protein. Related to Figure 1

(A) Top-ranked GO terms of DHA down-regulated phosphorylation sites in DHA-treated 129/C57BL6 mice.

(B) Illustration of Myc-GLUT4-mCherry fusion protein that was used in this study to report the cellular distribution of GLUT4. Myc (green fluorescence) was inserted into extracellular exposing part and mCherry (red fluorescence) was attached to the cytoplasmic exposing C-terminus end of GLUT4.

(C) Multi-cell view of DHA and EPA promote PDK1 and AKT2 membrane enrichment. PDK1 and AKT2 were ectopically expressed in 3T3-L1 cells. Scale bar, 50 μm.

(D) GLUT4 localization was altered by EPA, DHA and insulin. CHO-K1 cells that were successfully transfected with Myc-GLUT4-mCherry plasmid, the localization of the fusion protein were stained with immunofluorescence analysis for Myc and mCherry after cells were stimulated with DHA, EPA and insulin after serum starvation for 6 hours. Scale bar, 60 μm.

(E) DHA and EPA cause membrane enrichment and cytosolic depletion of PDK1, AKT2, and GLUT4. DHA, EPA, and insulin treated 3T3-L1 cells were fractionated to the membrane and cytosol fractions. The levels of AKT2, PDK1, GLUT4 in each fraction and whole cell lysate were determined.

(F) DHA and EPA can't induce membrane enrichment of GLUT4 in AKT2 KO CHO-K1 cells. CHO-K1 cells and AKT2 KO CHO-K1 cells were successfully transfected with Myc-GLUT4-mCherry plasmid, the localization of the fusion protein were stained with immunofluorescence analysis for Myc and mCherry after cells were stimulated with DHA and EPA after serum starvation for 6 hours. Scale bar, 100 μm.

(G) DHA and EPA activate AKT2. AKT activity was used to determine AKT2 purified from untreated and DHA-, EPA- and insulin-treated 3T3-L1 cells (n=3, mean ± SEM).

(H) DHA and EPA persistently retain AKT2 on membrane. The distribution of AKT2 on membrane and in cytoplasm was analyzed at time points after 3T3-L1 cells were treated with DHA, EPA or insulin(left), scale bar, 20 μm. The fraction of responded cells were quantified (right), (n=50, mean ± SEM)

(I and J) DHA and EPA dose-dependently activate PI3K signaling. The phosphorylation of AKT2 T308 and ASK160 T642 were analyzed for 3T3-L1 cells treated with different concentrations of DHA, DHA + Methyl-tryptophan **(I)** or EPA, EPA + Methyl-tryptophan **(J)**.

Figure S2

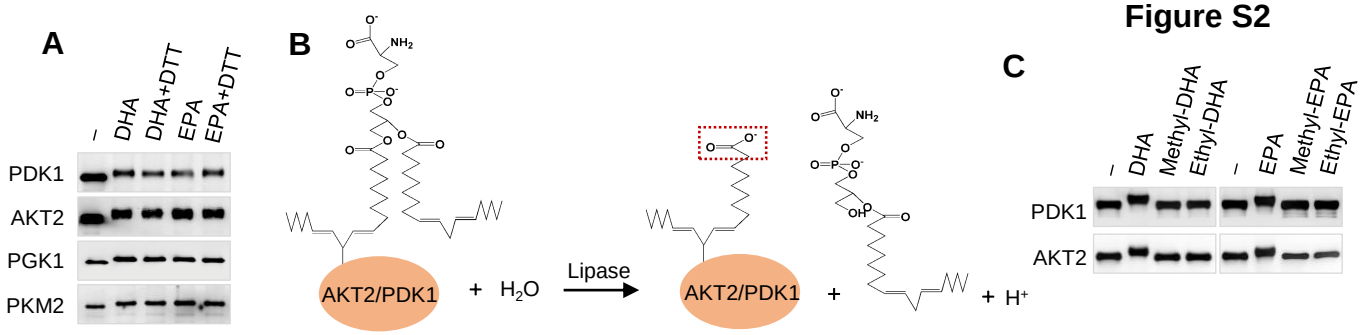

D

Peptide No.	Peptide Sequence	Peptide M.W.	Predicted LA Adduct M.W.	Predicted DHA Adduct M.W.	Predicted EPA Adduct M.W.	Adducts Formation
1	Ac-RDLIFKEREED	1491.63	1769.85	1817.85	1791.84	No
2	Ac-NLTCECKDLIYR	1512.76	1790.98	1838.98	1812.97	No
3	Ac-LPALKIREEL	1223.49	1501.71	1549.71	1523.70	No
4	Ac-LRITKLCGND	1174.39	1452.61	1500.61	1474.60	No
5	Ac-NIIFHTKPFYGG	1435.66	1713.88	1761.88	1735.87	No
6	Ac-PSYSQKSEDDSA	1355.34	1633.56	1681.56	1655.55	No
7	Ac-SMDDHKLSLDEL	1444.59	1722.81	1770.81	1744.80	No
8	Ac-PYVQMDKGVLQQG	1504.74	1782.96	1830.96	1804.95	No
9	Ac-QEMDKDDESL	1251.3	1529.52	1577.52	1551.51	No
10	Ac-PEMAAKLHPH	1172.38	1450.60	1498.60	1472.59	No
11	Ac-FTEGAFKDW*GYQLAR	1831.03	2109.25	2157.25	2131.24	Yes
11'	Ac-FTEGAFKDA*GYQLAR	1715.9	1994.12	2042.12	2016.11	No
12	Ac-EW*RPEKISDLQTQ	1671.84	1950.06	1998.06	1972.05	Yes
12'	Ac-EA*RPEKISDLQTQ	1556.7	1834.92	1882.92	1856.91	No
13	Ac-EAAW*KVTDEC	1192.29	1470.51	1518.51	1492.50	Yes
13'	Ac-EAAA*KVTDEC	1078.1	1356.32	1404.32	1378.31	No

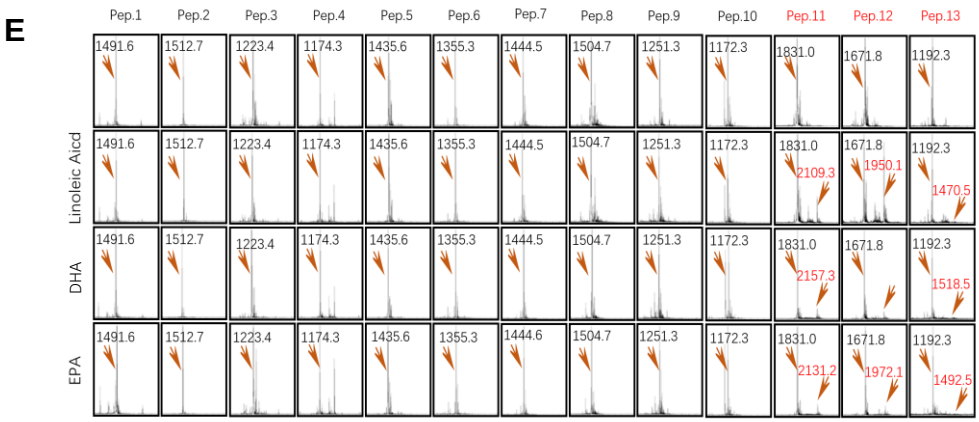

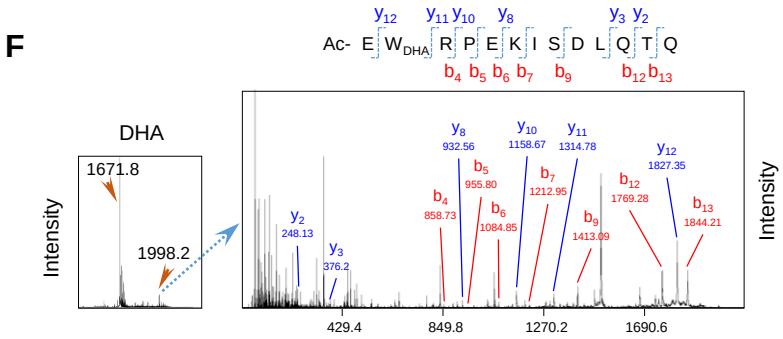

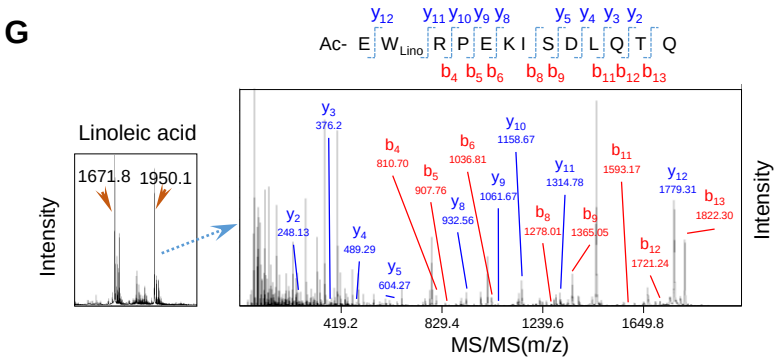

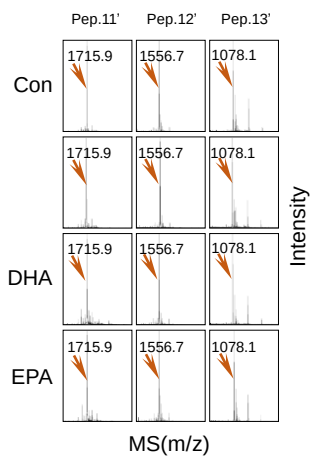

Figure S2. Methylene bridge-containing PUFAs react with tryptophan. Related to Figure 2

(A) DHA and EPA induce migration shift of proteins. Proteins before and after incubated with DHA or EPAA under absence and presence of DTT in the reaction solution were resolved in SDS PAGE.

(B) Schematic diagram for lipase treatment to expose carboxyl groups of PS. The exposed carboxyl group was marked with red rectangle.

(C) Carboxyl-neutralized DHA and EPA failed to induce mobility shift of AKT2 and PDK1 in vitro. The abilities of DHA, EPA, methyl-DHA, ethyl-DHA, methyl-EPA and ethyl-EPA to induce PDK1 and AKT2 mobility shifts in vitro were tested.

(**D**) The reactivity of N-terminus acetylated synthetic peptides to DHA, EPA and linoleic acid. Sequences, molecular weights and molecular weights of predicted adducts of synthetic peptides used for searching the reactive residues are shown.

(**E**) The formation of acylated products (red colored m/z) between peptides and with linoleic acid, DHA and EPA was assayed by MS.

(F and G) The formation of DHA acylated (**F**) and linoleic acylated (**G**) peptides were detected by MS (m/z) and confirmed by MS/MS (fragmentation) analysis. Identified y (blue) and b (red) fragments and their m/z were marked.

(H) The formation of acylated products (red colored m/z) between peptides (#11', #12'and #13') and with linoleic acid, DHA and EPA was assayed by MS.

Figure S3

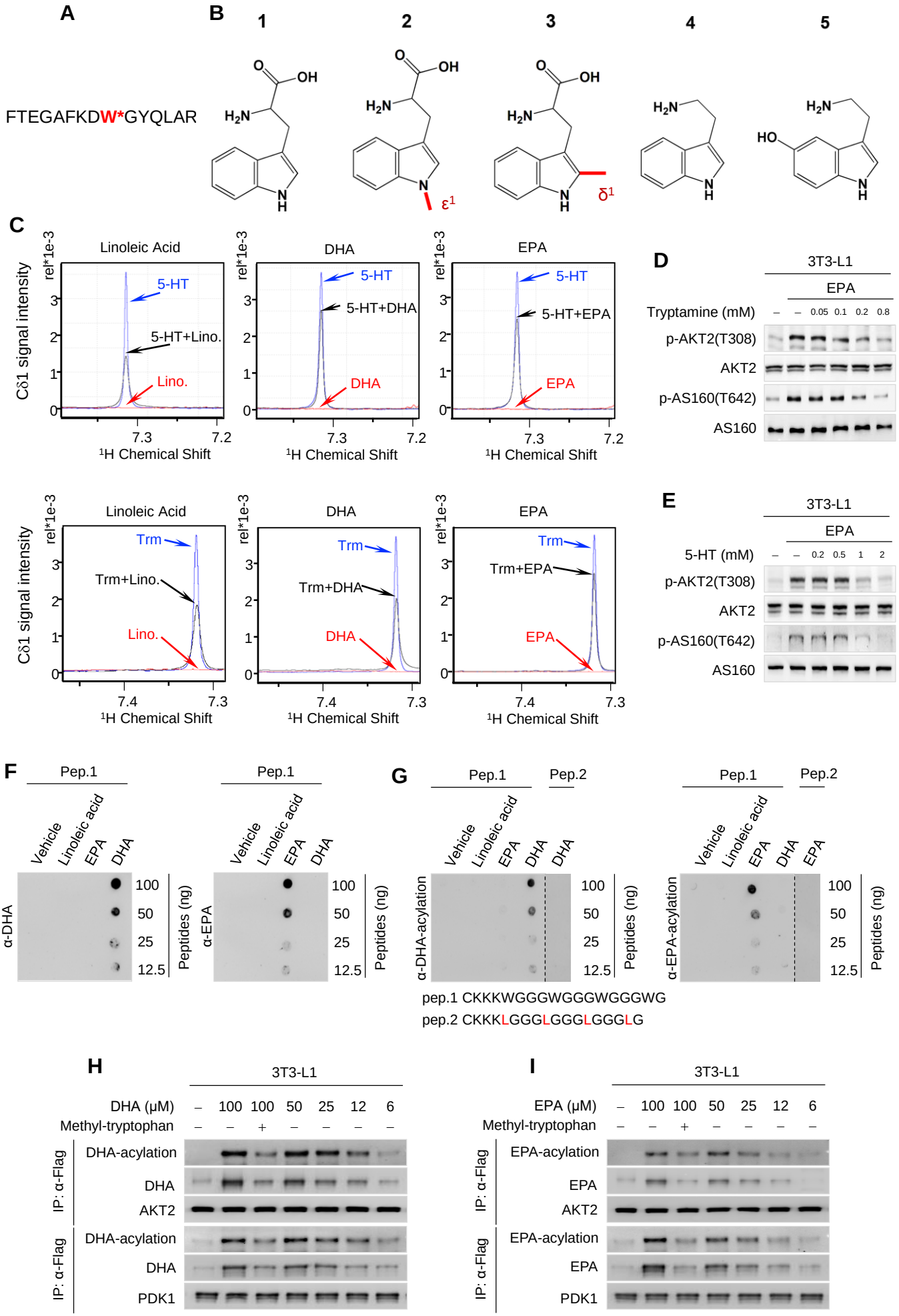
A
FTEGAFKDW*GYQLAR
B
1
2
3
4
5
ε1
δ1
C
Linoleic Acid
DHA
EPA
Cδ1 signal intensity
rel*1e-3
5-HT
5-HT+Lino.
Lino.
5-HT+DHA
DHA
5-HT+EPA
EPA
1H Chemical Shift
Trm
Trm+Lino.
Trm+DHA
Trm+EPA
D
3T3-L1
EPA
Tryptamine (mM)
– – 0.05 0.1 0.2 0.8
p-AKT2(T308)
AKT2
p-AS160(T642)
AS160
E
3T3-L1
EPA
5-HT (mM)
– – 0.2 0.5 1 2
p-AKT2(T308)
AKT2
p-AS160(T642)
AS160
F
Pep.1
Vehicle
Linoleic acid
EPA
DHA
α-DHA
α-EPA
100
50
25
12.5
Peptides (ng)
G
Pep.1
Pep.2
DHA
α-DHA-acylation
α-EPA-acylation
pep.1 CKKKWGGGWGGGWGGGWG
pep.2 CKKKLGGGLGGGLGGGLG
H
3T3-L1
DHA (μM)
– 100 100 50 25 12 6
Methyl-tryptophan
– – + – – – –
IP: α-Flag
DHA-acylation
DHA
AKT2
PDK1
I
3T3-L1
EPA (μM)
– 100 100 50 25 12 6
Methyl-tryptophan
– – + – – – –
IP: α-Flag
EPA-acylation
EPA
AKT2
PDK1

Figure S3, Cδ1 in tryptophan is the site for methylene-bridge acylation, Related to Figure 3

(A) The amino acids sequence of peptide that were used to verify reactivities of tryptophan and tryptophan derivatives.

(B) The structures of tryptophan and its derivatives or analogs used in this study. (1), tryptophan; (2), Nε1 methyl-blocked tryptophan; (3) Cδ1 methyl-blocked tryptophan; (4) tryptamine (Trm) and (5) 5-hydroxy-tryptamine (5-HT).

(C) Cδ1-containing tryptophan analogs 5-hydroxy-tryptamine and tryptamine reacted with Linoic acid, DHA and EPA. The NMR signals of Cδ1 of 5-hydroxy-tryptamine (upper) and tryptamine (lower) was each decreased by Linoic acid, DHA and EPA incubation, respectively.

(D and E) AKT signalling activation by EPA was reversed by tryptamine **(D)** and 5-hydroxy-tryptamine (5-HT) **(E)**. The levels of p-AKT2(T308) and p-AS160(T642) were determined in 3T3-L1 cells cultured in media supplemented with EPA, EPA/ tryptamine, or EPA/5-HT.

(F and G) The reactivity of α-DHA and α-EPA (**F**) and specific DHA- or EPA-acylation (**G**) antibodies to synthetic that were treated with indicated PUFAs were analyzed by dot blot.

(H and I) DHA and EPA dose-dependently increased acylations on AKT2 and PDK1. The DHA- **(H)** or EPA-acylation **(I)** of AKT2 or PDK1 ectopically expressed in 3T3-L1 cells with or without DHA/EPA treatments under absence or presence of Me-tryptophan was detected with α-DHA, α-EPA, DHA- or EPA-acylation.

Figure S4

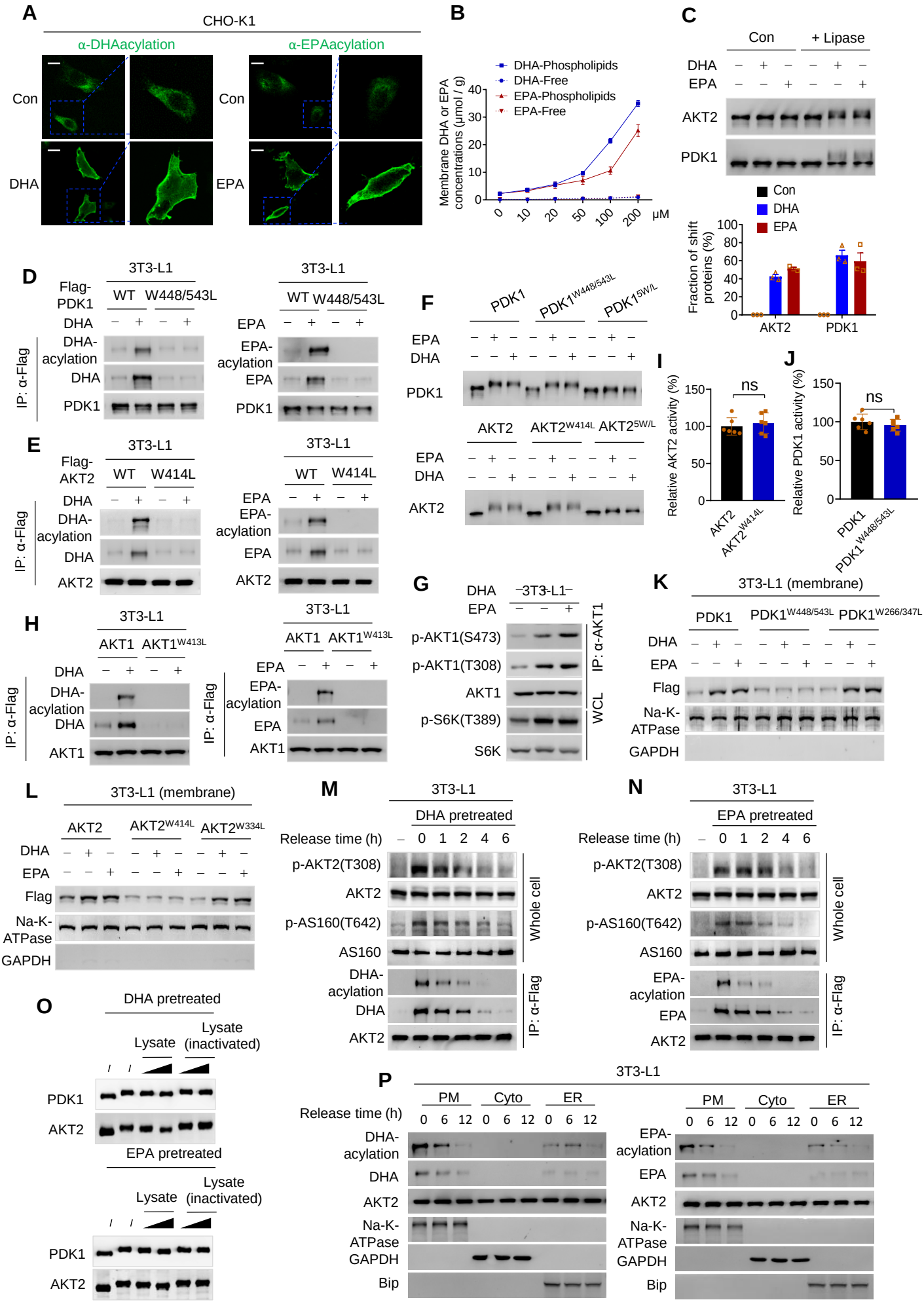
A
CHO-K1
α-DHAacylation
α-EPAacylation
Con
DHA
EPA
B
DHA-Phospholipids
DHA-Free
EPA-Phospholipids
EPA-Free
Membrane DHA or EPA concentrations (μmol / g)
μM
C
Con
+ Lipase
DHA
EPA
AKT2
PDK1
Fraction of shift proteins (%)
D
3T3-L1
Flag-PDK1
WT
W448/543L
IP: α-Flag
DHA-acylation
EPA-acylation
E
Flag-AKT2
W414L
F
PDK1
PDK1W448/543L
PDK1 5W/L
AKT2
AKT2W414L
AKT2 5W/L
G
p-AKT1(S473)
p-AKT1(T308)
p-S6K(T389)
S6K
IP: α-AKT1
WCL
H
AKT1
AKT1W413L
I
Relative AKT2 activity (%)
ns
J
Relative PDK1 activity (%)
K
3T3-L1 (membrane)
PDK1W266/347L
Flag
Na-K-ATPase
GAPDH
L
AKT2W334L
M
DHA pretreated
Release time (h)
p-AKT2(T308)
p-AS160(T642)
AS160
Whole cell
N
EPA pretreated
O
Lysate
Lysate (inactivated)
P
PM
Cyto
ER
Bip

Figure S4. W448 and W543 of PDK1 and W414 of AKT2 are acylated by DHA and EPA in cells. Related to Figure 4

(A) DHA- and EPA -acylation signals enriched in cytoplasmic membrane. Living cell imaging was used to probe protein DHA- (left) and EPA (right) -acylation signals in CHO-K1 cells. scale bar, 40 μm.

(**B**) DHA and EPA predominantly exist as phospholipids in cell membrane. The membrane levels of free DHA, freee EPA, DHA conjugated phospholipids and EPA conjugated phospholipids were determined 2 hours after the cells were treated with either DHA or EPA, (n=3, mean ± SEM).

(**C**) DHA and EPA induces AKT2 and PDK1 mobility shift. AKT2-flag and PDK1-flag were ectopically expressed and treated with DHA/EPA in 3T3-L1. Purified AKT2 and PDK1 were treated by lipase, then the proteins were resolved in SDS-PAGE. The fraction of shift proteins were quantified (right), (n=3, mean ± SEM).

(**D-E**) Removal of in vivo DHA-/EPA-acylation sites abrogates DHA and EPA to acylate PDK1 and AKT2. The PDK1-flag, AKT2-flag, PDK1$^{W448/543L}$-flag and AKT2^{W414L}-flag were ectopically expressed in 3T3-L1 or DHA/EPA-treated 3T3-L1 cells. The DHA-/EPA-acylation levels (Antibodies used here were described in Fig S6) of PDK 1 and PDK1$^{W448/543L}$ (**D**), and AKT2 and AKT2^{W414L} (**E**) were detected.

(**F**) The ability of DHA and EPA to cause mobility shift of PDK1 and its mutants (upper) and AKT2 and its mutants (lower) were analyzed *in vitro*.

(**G-H**) DHA and EPA regulates AKT1 signaling. The phosphorylation of AKT1 S473 and T308, and S6K T389 (**G**) and the DHA-/EPA-acylation levels (Antibodies used here were described in Fig S6) of AKT1 and AKT1^{W413L} (**H**) were detected in 3T3-L1 cells with or without DHA or EPA treatments.

(I and J) AKT2^{W414L} (**I**) and PDK1$^{W448/543L}$ (**J**) are catalytically active. The AKT2-flag, AKT2^{W414}-flag, PDK1-flag and PDK1$^{W448/543L}$-flag were purified from 3T3-L1 cells by flag-beads and then the activity of the ectopically proteins were detected, (n=3, mean ± SEM).

(K and L) The membrane contents of PDK1, PDK1$^{W448/543L}$ and PDK1$^{W226/347L}$ (**K**), and AKT2, AKT2^{W414L} and AKT2^{W334L} (**L**) were analyzed with or without DHA or EPA treatments.

(M and N) DHA- and EPA-acylation is reversible. The activation of AKT2 signaling and the acylation of AKT2 by DHA (**M**) and EPA (**N**) were monitored at different time after their removal from culture media.

(O) Cell lysate reverse DHA- and EPA-acylation. The ability of lysate and heat-inactivated 3T3-L1 lysate to reverse mobility of DHA-(left) and EPA-induced (right) Flag beads affinity purified PDK1 and AKT2 proteins from 3T3-L1 cells were analyzed 1 hr after treatments.

(P) DHA- and EPA-acylated AKT2 distributes in membranes and are reversible. 3T3-L1 cells were treated with DHA or EPA followed by DHA or EPA removal. Acylated AKT2 was detected in cytoplasm membrane (PM) cytoplasm and endoplasmic reticulum (ER) over time.

Figure S5

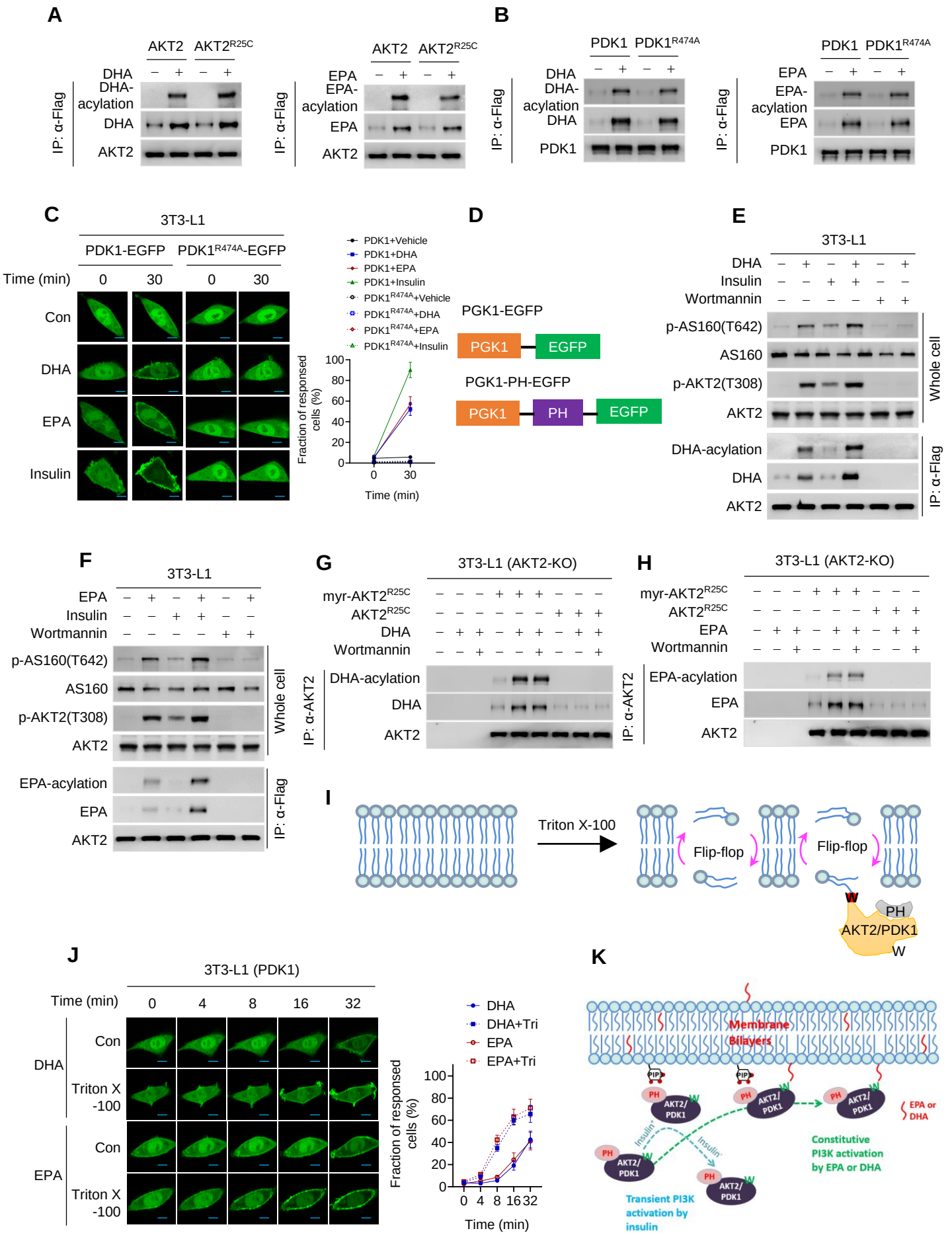
A
AKT2
AKT2R25C
DHA
DHA-acylation
AKT2
IP: α-Flag
EPA
EPA-acylation
B
PDK1
PDK1R474A
PDK1
C
3T3-L1
PDK1-EGFP
PDK1R474A-EGFP
Time (min)
Con
DHA
EPA
Insulin
PDK1+Vehicle
PDK1+DHA
PDK1+EPA
PDK1+Insulin
PDK1R474A+Vehicle
PDK1R474A+DHA
PDK1R474A+EPA
PDK1R474A+Insulin
Fraction of responsed cells (%)
D
PGK1-EGFP
PGK1
EGFP
PGK1-PH-EGFP
PH
E
3T3-L1
Insulin
Wortmannin
p-AS160(T642)
AS160
p-AKT2(T308)
Whole cell
F
G
3T3-L1 (AKT2-KO)
myr-AKT2R25C
H
I
Triton X-100
Flip-flop
W
AKT2/PDK1
J
3T3-L1 (PDK1)
Triton X -100
DHA+Tri
EPA+Tri
K
Membrane Bilayers
PIP3
Insulin
EPA or DHA
Constitutive PI3K activation by EPA or DHA
Transient PI3K activation by insulin

Figure S5. Membrane anchoring facilitate proteins to be acylated by DHA and EPA. Related to Figure 5.

(A-B) PH-domain defective AKT2 and PDK1 are acylated in vitro. The in vitro acylation of AKT2 and AKT2^{R25C} (**A**), and PDK1 and PDK1^{R474A} (**B**) were analyzes after they were incubated with either DHA or EPA.

(**C**) PH-domain defective PDK1^{R474A} can not be induced to membrane by either DHA or EPA. Immunofluorescence analysis was employed to 3T3-L cells before and after DHA, EPA and insulin treatments (left), scale bar, 20 μm. The fraction of response cells were quantified (right), (n=50, mean ± SEM)

(**D**)Illustration of fusing a PH domain into PGK1.

(E-F) Increasing and Inhibiting PIP3 production enhanced and prevented DHA and EPA to activate PI3K signaling respectively. The ability of DHA **(E)** and EPA **(F)** to activate PI3K signaling and acylate AKT2 in 3T3-L1 cells were analyzed under absence or presence of insulin or wortmannin.

(G-H) Membrane bound AKT2 is highly acylated by DHA and EPA. The acylation by DHA (**G**) or EPA (**H**) to myr-AKT2^{R25C} and AKT2^{R25C} were analyzed in 3T3-L1 cells under with or without wortmannin treatments.

(I) Illustration of how Triton-X100-facilitated flip-flop motion expose membrane embedded acyl ends to cytoplasmic proteins.

(J) Triton-X100 facilitates PDK1 membrane recruiting by DHA and EPA. Confocal live-cell fluorescence images were obtained for PDK1-expressing 3T3-L1 cells that were treated with DHA or EPA with or without Triton X-100 (10 nM). Triton X-100 was supplemented prior to EPA and DHA treatment for 1 h. Scale bar, 20 μm. The fraction of response cells were quantified (right) , (n=50, mean ± SEM).

(K) Illustration of how DHA and EPA to activate PI3K signaling by recruiting AKT2/PDK1 onto membrane.

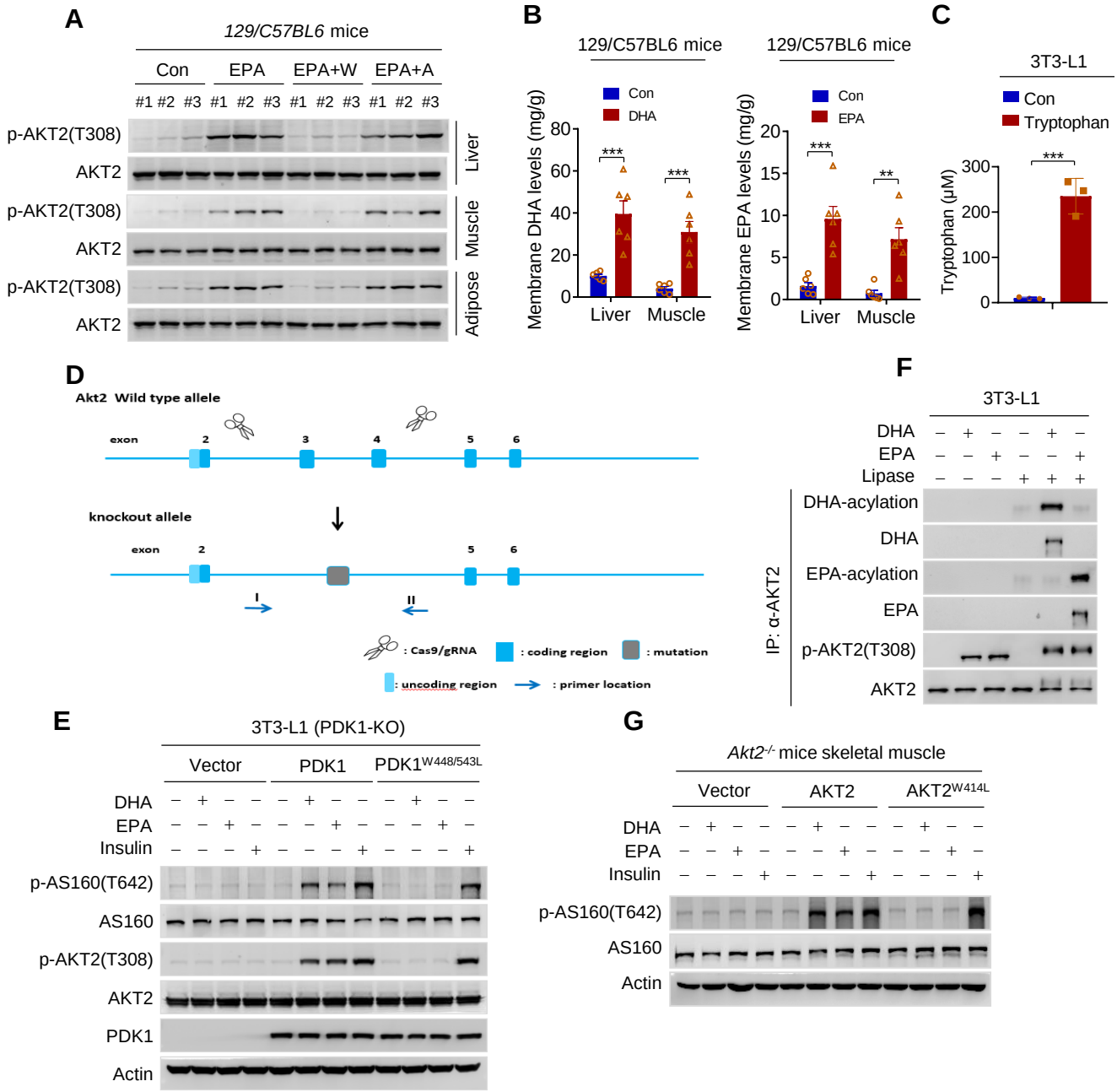

Figure S6. Tryptophan DHA-/EPA-acylation activates PI3K signaling. Related to Figure 6

(**A**) EPA activates PI3K signaling in mice via tryptophan EPA-acylation. The phosphorylation of AKT2 were detected in mice liver, muscle and adipocytes before and after the 129/C57BL6 mice were treated with EPA, EPA with tryptophan and EPA with alanine.

(B) Liver and muscle membrane levels of DHA (left) and EPA (right) were increased by DHA and EPA feeding, (n=6, mean ± SEM).

(C) Intracelluar tryptophan levels in 3T3-L1 cells were elevated by methyl-tryptophan treatment, (n=3, mean ± SEM).

(D) Scheme of CRISPR-mediated *Akt2* knockout in 129/C57BL6 mice.

(**E**) AKT2 phosphorylation was irresponsive to DHA, EPA and insulin under absence of PDK1. AKT2 and AS160 phosphorylation was detected for PDK1-KO 3T3-L1 cells, and PDK1-KO 3T3-L1 cells with either wildtype or $PDK1^{W448/543L}$ putback.

(**F**) AKT2 phosphorylation is associated with DHA-/EPA-acylation. The phosphorylation and DHA-/EPA-acylation of purified AKT2 were detected after lipase treatment.

(G) AKT2 is required for DHA and EPA to stimulate p-AS160. The levels of p-AS160(T642) were detected in the skeletal muscle of DHA, EPA or insulin treated $Akt2^{-/-}$ mice overexpressed with vector, AKT2 and $AKT2^{W414L}$.

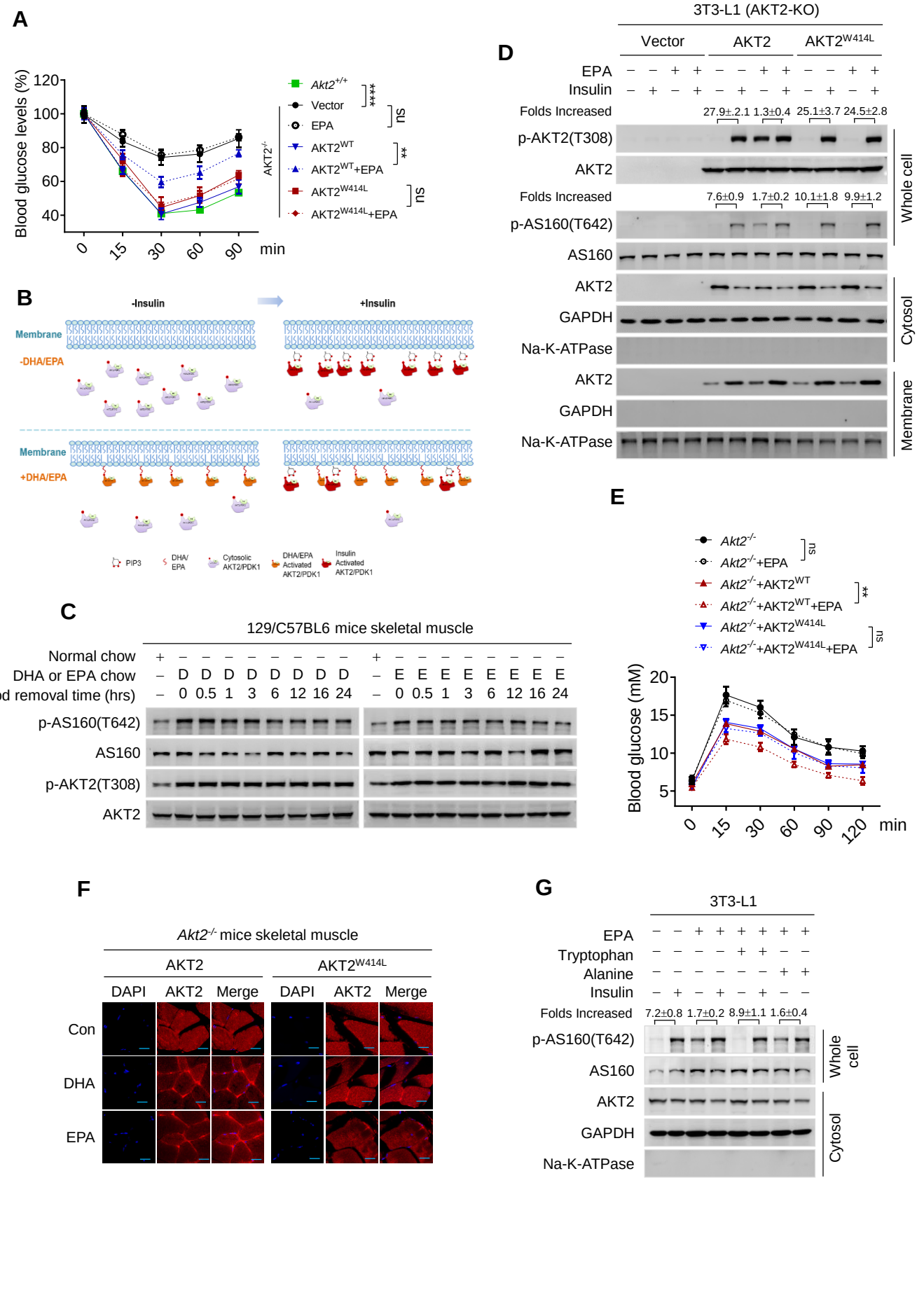
A
Blood glucose levels (%)
120
100
80
60
40
0
15
30
60
90
min
Akt2+/+
Vector
EPA
AKT2WT
AKT2WT+EPA
AKT2W414L
AKT2W414L+EPA
AKT2-/-
****
ns
**
ns
B
-Insulin
+Insulin
Membrane
-DHA/EPA
Membrane
+DHA/EPA
PIP3
DHA/EPA
Cytosolic AKT2/PDK1
DHA/EPA Activated AKT2/PDK1
Insulin Activated AKT2/PDK1
C
129/C57BL6 mice skeletal muscle
Normal chow
DHA or EPA chow
Food removal time (hrs)
p-AS160(T642)
AS160
p-AKT2(T308)
AKT2
D
3T3-L1 (AKT2-KO)
Vector
AKT2
AKT2W414L
EPA
Insulin
Folds Increased
27.9±.2.1 1.3±0.4 25.1±3.7 24.5±2.8
p-AKT2(T308)
AKT2
Folds Increased
7.6±0.9 1.7±0.2 10.1±1.8 9.9±1.2
p-AS160(T642)
AS160
AKT2
GAPDH
Na-K-ATPase
AKT2
GAPDH
Na-K-ATPase
Whole cell
Cytosol
Membrane
E
Akt2-/-
Akt2-/-+EPA
Akt2-/-+AKT2WT
Akt2-/-+AKT2WT+EPA
Akt2-/-+AKT2W414L
Akt2-/-+AKT2W414L+EPA
ns
**
ns
Blood glucose (mM)
20
15
10
5
0
15
30
60
90
120
min
F
Akt2-/- mice skeletal muscle
AKT2
AKT2W414L
DAPI
AKT2
Merge
DAPI
AKT2
Merge
Con
DHA
EPA
G
3T3-L1
EPA
Tryptophan
Alanine
Insulin
Folds Increased
7.2±0.8 1.7±0.2 8.9±1.1 1.6±0.4
p-AS160(T642)
AS160
AKT2
GAPDH
Na-K-ATPase
Whole cell
Cytosol

Figure S7. DHA and EPA compete insulin signaling by competing cytosolic AKT2/PDK1 availability, Related to Figure 7

(A) EPA acylation induced insulin resistance. Insulin tolerance test were performed in EPA pre-treated Akt2$^{-/-}$ 129/C57BL6 mice and Akt2$^{-/-}$ 129/C57BL6 mice overexpressing AKT2^{WT} or AKT2^{W414L} (n = 6, mean ± SEM).

(B) Schematic diagram of DHA and EPA inducing insulin resistance by depleting cytoplasmic AKT2/PDK1.

(C) DHA and EPA effects on AKT signaling activation last for over 24 hrs after treatment. The phosphorylation levels of AS160 and AKT2 was monitored in mice at time points as indicated after they had received DHA or EPA treatments.

(D) Overexpression of AKT2, but not AKT2^{W414L}, enabled EPA to activate AKT signaling pathway in Akt2$^{-/-}$ mice. The levels of p-AS160(T642), p-AKT2(T308), the cytoplasmic levels of AKT2 and the membrane levels of AKT2 were detected in the skeletal muscle of Akt2$^{-/-}$ mice overexpressed with vector, AKT2 and AKT2^{W414L}. Insulin was added to EPA-pretreated cells. Quantification was represented as mean ± SEM based on three independent repeats.

(E) AKT2 is required for EPA to decrease blood glucose in mice. Glucose tolerance tests were performed to *Akt2*$^{-/-}$ mice and *Akt2*$^{-/-}$ mice forced expressing either AKT2 or AKT2^{W414L}, under absence or presence of EPA treatments (n = 6, mean ± SEM).

(F) Overexpression of AKT2 or AKT2^{W414L} restored cytoplasmic presence of AKT2 in skeletal muscles of Akt2$^{-/-}$ mice. The distribution of AKT2 in the skeletal muscle of Akt2$^{-/-}$ mice overexpressed with vector, AKT2 and AKT2^{W414L} were analysed by immunofluorescence. Scale bar, 50 μm.

(G) EPA tryptophan-reversibly deplete cytosolic AKT2 and induce p-AS160 (T642). The levels of p-AS160(T642) in the whole cell lysate and AKT2 in the cytosol were determined in 3T3-L1 cells. Quantification was represented as mean ± SEM based on three independent repeats.